

Measurement of characteristic feature of cavitation flows of He I and He II

Harada K., Tsukahara R., and Murakami M.

Institute of Engineering Mechanics and Systems, University of Tsukuba, Tsukuba, 305-8573, Japan

In the present experimental study cavitation phenomena in both He I and He II flows were investigated through the pressure and temperature measurements and the application of optical visualization. The cavitation flow is generated in the downstream region of a Venturi channel driven by contracting the metal bellows. The cavitating flows can be observed through the optical windows of the cryostat. Tests were carried out for both He II and He I. The pressure loss and the temperature drop caused by cavitation are measured in a wide range of the flow velocity. The spatial distribution of the cavitation bubble velocity is also measured by the application of PIV (Particle Image Velocimetry) technique.

INTRODUCTION

Use of cryogenic fluids such as liquid helium has been expanded in large scale cryogenic plants relating to aerospace and superconductivity applications. There occurred a serious accident of the H-II rocket in 1999 of which cause was cavitation in the liquid hydrogen turbo-pump. However, there have been a little cavitation researches of cryogenic fluids [Reference 1, 2, 3]. ! It is, thus, the purpose of this research to experimentally study cavitation flow of cryogenic fluids, in particular of liquid helium. We measured the temperature drop induced by cavitation and the pressure loss as a pressure difference between the upstream and downstream points of the channel in a wide range of the flow velocity. Visualization pictures were also taken for both cavitating He I and He II flows for the purpose of visualization and PIV measurement.

EXPERIMENTAL SET-UP

A schematic illustration of the key area of the experimental set-up is shown in Fig. 1. This section composed of a Venturi channel, a metal bellows, a pressure transducer and a temperature sensor is immersed in liquid helium. The flow is generated by the metal bellows pump. The detail of the two-dimensional Venturi channel is represented in Fig. 2. Cavitation is generated in the downstream region of the Venturi channel, which consists of two pieces of thin stainless steel plate shaped into a Venturi profile placed between two parallel plates of quartz glass. It is of a rectangular cross section with a thickness of 3 mm between the glass plates, a maximum width of 15 mm at the downstream exit, and a minimum width of 5 mm at the throat. The velocity of the flow was kept constant during each experiment. The maximum velocity was $V_t=30.70$ m/s at the throat. The cavitating flow can be observed through the cryostat windows of 60 mm-diameter and recorded with a high-speed video camera or a digital still camera. The absolute pressure transducer was used to measure the pressure loss between the upstream chamber and the outside of the channel. A thin film resistance temperature sensor (Cernox) fixed at the tip of the plastic probe was inserted into the downstream diverging section at the center of channel below the throat by 25 mm

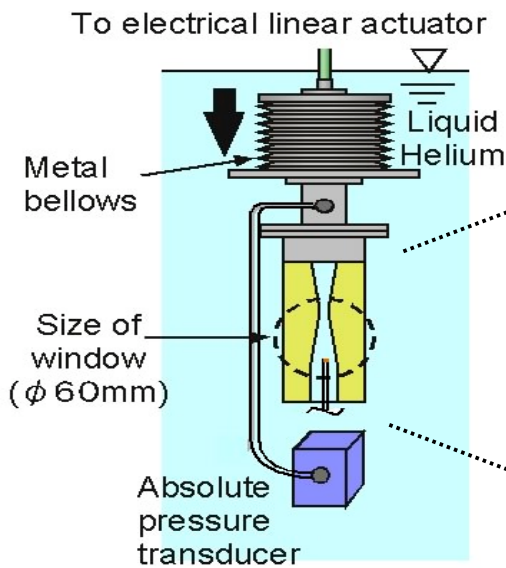


Fig. 1 The schematic illustration of the key area of experimental set-up

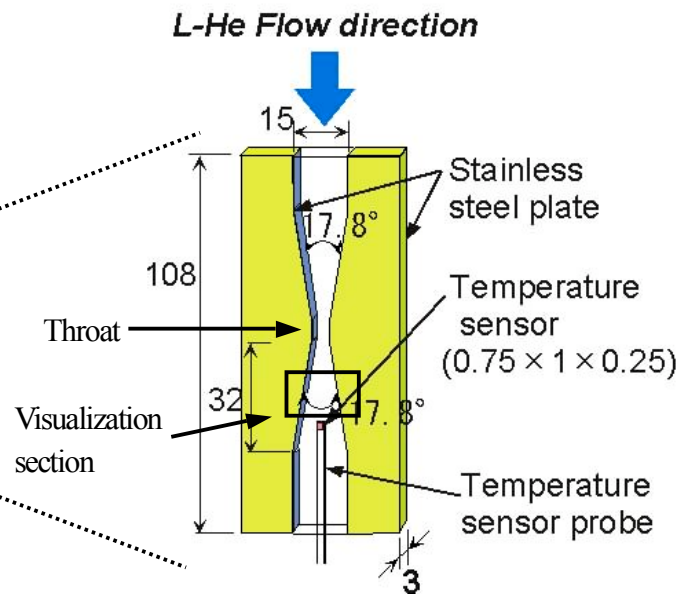


Fig. 2 The detail of two-dimensional Venturi channel

RESULTS AND DISCUSSION

Pressure loss data

The relation between the pressure loss, P_{loss} , and the velocity at the throat, V_t , is presented in Fig. 3 for the case of fully developed cavitating flows. It is seen that there is a difference in the magnitude of the pressure loss between He I and He II. In the case of He II, the data are almost independent of the temperature, but in the case of He I, temperature dependency is clearly recognized. It is considered that the difference in the void fraction causes the difference in P_{loss} between He I and He II. According to the visualization study by a high speed camera, it was clear that cavitation flows of He I were more intermittent than those of He II. It is indicated, consequently, that the void fraction of He I flow is smaller than that of He II in an averaged sense. The pressure loss becomes large as the bath temperature drops toward the λ -temperature, T_λ , in the case of He I. The fact that the pressure loss curve for 2.2 K coincides with the He II curve can be explained by the λ -transition from He I to He II as a result of cavitation bubble formation. It is necessary to measure the void fraction in order to quantitatively understand the difference in the pressure loss between He I and He II.

Cavitation number plot

The P_{loss} data include the effect of the saturated vapor pressure as a strong function of temperature. Elimination of the effect of the saturated vapor pressure is more appropriate for more discussion. So the pressure loss data are rearranged in terms of the cavitation number σ defined by $2[p_\# - p_v(T_\#)] / \rho V_t^2$. The cavitation inception and the magnitude of cavitation can be also quantitatively investigated in terms of σ . Here $p_\#$ and $p_v(T_\#)$ are the pressures in the upstream chamber and of the saturated vapor at the liquid temperature $T_\#$, and ρ is the liquid density. The relation between σ and V_t is presented in Fig. 4 for a wide range of the velocity, V_t . It is distinguishable there are two branches in the data plot, non-cavitating and cavitating branches. Along the cavitating branch of He II σ is nearly constant independently of V_t though it is weakly dependent on $T_\#$. It was also seen that the magnitude of σ is clearly different between He I and He II in the cavitation inception region with small V_t and both σ values for He I and He II close to each other in the fully developed case. In the case of He II flows, the cavitation inception causes sudden jump in cavitation number. However, in He I flows, cavitation number rises continuously irrespectively of cavitation inception. It seems the critical

value V_t for the inception is not definitely decided between 5 and 10 m/s, but it is rather sensitive to disturbances.

Temperature drop data

The temperature drop, ΔT , from the initial temperature caused by cavitation is plotted against V_t in Fig. 7. It is seen that the He II branches can be clearly distinguished from the He I branch. In the case of He I, the temperature drop rapidly increases with the increase of V_t . However, in the case of He II, the temperature drop increases more moderately. The occurrence of the cavitation-induced λ -transition is clearly recognized by the sudden change of the gradient of the data in the cases of T, 2.2 K and 2.3 K. This was fully reasoned in Ishii's articles [Reference 2,3].

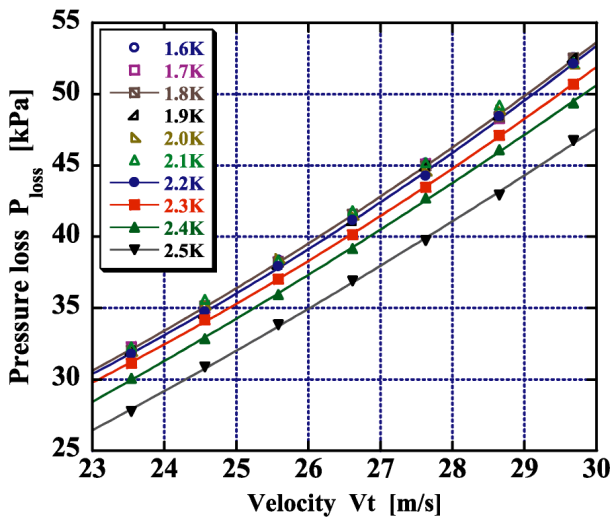


Fig. 3 The relation between the velocity, V_t and the pressure loss, P_{loss} across the throat

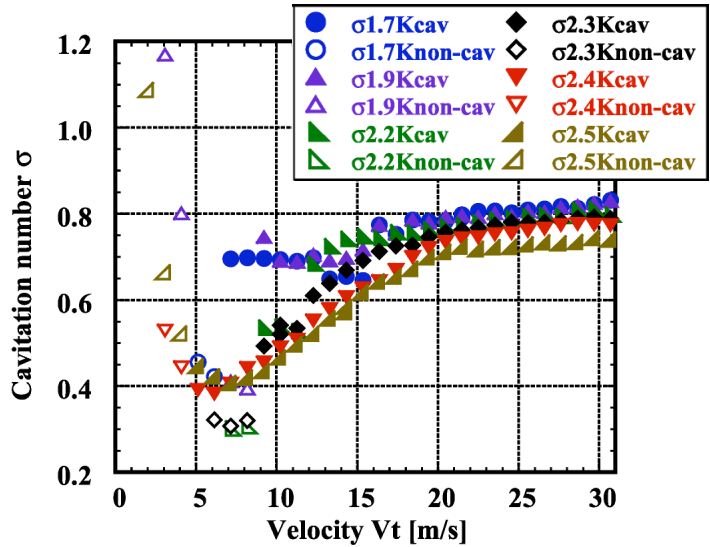
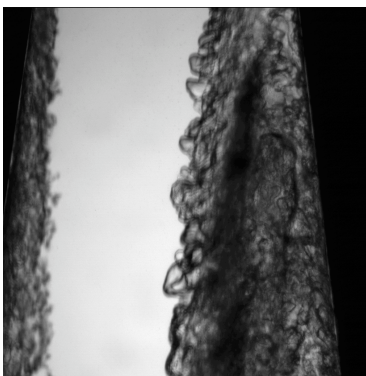


Fig. 4 Data plot of the cavitation number, σ , versus the velocity, V_t , at the throat



T=1.90K (He II)



T=2.20K (He I)



T=2.50K (He I)

Fig. 5 Pictures of the cavitation flow of He I and He II for $V_t=12.28$ m/s. The visualization area is a part of the Venturi channel(10 \$ 10 mm) at 11 mm downstream of the throat indicated by a square in Fig. 2.

Visualization and PIV results

The comparison of the visualization pictures of cavitation flows of He I and He II is presented in Fig. 5. Large scale vapor bubbles are seen in the He II flow at 1.9 K, while massive minute bubbles like dark cloud are seen in He I flow at 2.50 K. The image at 2.20 K seems to be a mixture of them. It is because bubbly flow was partly converted into He II as a result of temperature drop. It was seen from the photographs taken by the high speed camera that cavitation flows of He I were highly intermittent, on the other hand He II flows were rather steady and exhibit definite formation of separation shear layer. The PIV technique is successfully applied to cavitating flows of He I and He II. Cavitation bubble velocity field is shown in Fig. 6 which is the PIV result for the picture at 2.20 K shown in the middle of Fig. 5

It is found that the PIV result for He II cavitating flow, which is not shown in this paper due to lack of space, is also different from that for He I as recognized by the visualization pictures. It is suggested by the picture of He I cavitating flow shown in Fig. 5 that large scale vortex shedding causes flow intermittency. The PIV result also evidently shows the flow structure with large scale vortex shedding.

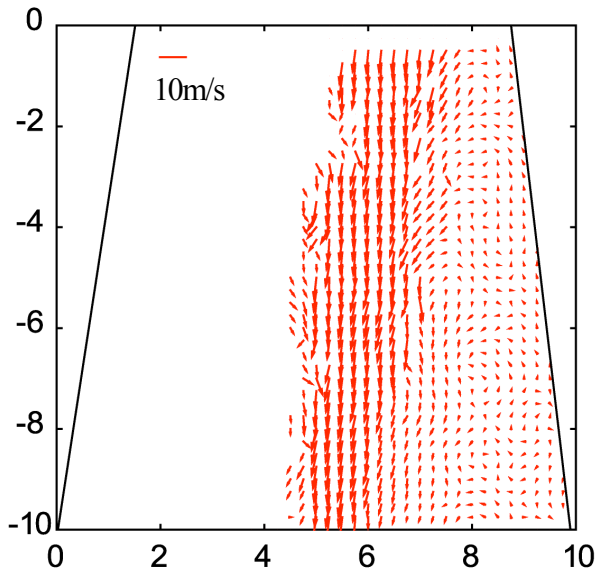


Fig. 6 PIV result of He II cavitating flow at 2.50K measured in the downstream flow field (10 × 10mm)

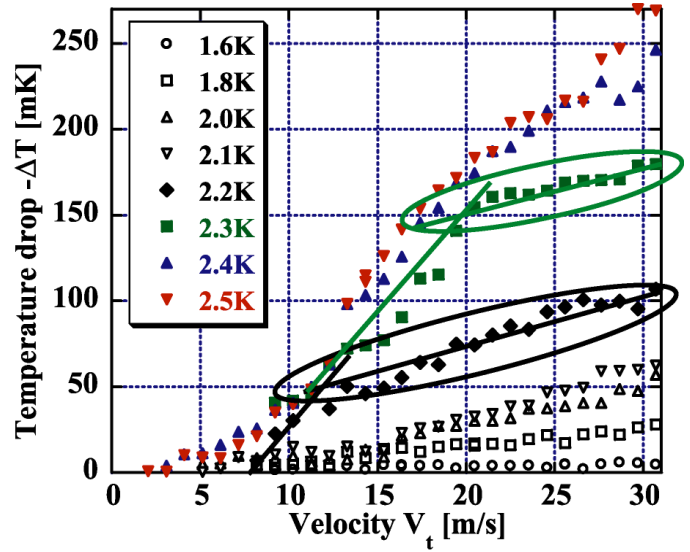


Fig. 7 The temperature drop plotted as a function of V_t

CONCLUSIONS

From this experimental study through the optical visualization and the measurements of the pressure and temperature, the following conclusions are drawn.

1. It is seen that there is a difference in the magnitude of the pressure loss between He I and He II. In the case of He II, the data are almost independent of the temperature, but in the case of He I, temperature dependency is clearly recognized.
2. In the case of He II flows, the cavitation inception causes sudden jump in cavitation number. However, in He I flows, cavitation number rises continuously irrespectively of cavitation inception.
3. The occurrence of the cavitation induced λ -transition is clearly recognized by sudden transfer to He II branch.
4. Large scale vapor bubbles are seen in the He II flow, while massive minute bubbles like dark cloud are seen in He I flow.
5. It was confirmed that bubbly flow in He I was partly converted into He II as a result of temperature drop.
6. It was seen from the photographs taken by the high speed camera that cavitation flows of He I were highly intermittent, while He II flows were rather steady and exhibit a definite formation of separation shear layer.
7. The PIV technique is successfully applied to cavitating flows of He I and He II. It was found that the PIV result for He II cavitating flow is different from that for He I as recognized by the visualization pictures.

REFERENCES

1. T. Ishii and M. Murakami, Comparison of cavitation flows in He I and He II, *Cryogenics* (2003) 43 507-514
2. Jun Ishimoto and Kenjiro Kamijo, Numerical simulation of cavitating flow of liquid helium in venturi channel, *Cryogenics* (2003) 43 9-17
3. Takashi ISHI, Masahide MURAKAMI, Temperature Measurement and Visualization Study of Liquid Helium Cavitation Flow Through

